Equilibrium and Kinetic Folding of a α-Helical Greek Key Protein Domain: Caspase Recruitment Domain (CARD) of RICK

Yun-Ru Chen and A. Clay Clark*

Department of Molecular and Structural Biochemistry, North Carolina State University, Raleigh, North Carolina 27695

Received January 15, 2003

ABSTRACT: We have characterized the equilibrium and kinetic folding of a unique protein domain, caspase recruitment domain (CARD), of the RIP-like interacting CLARP kinase (RICK) (RICK-CARD), which adopts a α-helical Greek key fold. At equilibrium, the folding of RICK-CARD is well described by a two-state mechanism representing the native and unfolded ensembles. The protein is marginally stable, with a ΔG^{H_2O} of 3.0 ± 0.15 kcal/mol and an *m*-value of 1.27 ± 0.06 kcal mol^{-1} M^{-1} (30 mM Tris-HCl, pH 8, 1 mM DTT, 25 °C). While the *m*-value is constant, the protein stability decreases in the presence of moderate salt concentrations (below 200 mM) and then increases at higher salt concentrations. The results suggest that electrostatic interactions are stabilizing in the native protein, and the favorable Coulombic interactions are reduced at low ionic strength. Above 200 mM salt, the results are consistent with Hofmeister effects. The unfolding pathway of RICK-CARD is complex and contains at least three non-native conformations. The refolding pathway of RICK-CARD also is complex, and the data suggest that the unfolded protein folds via two intermediate conformations prior to reaching the native state. Overall, the data suggest the presence of kinetically trapped, or misfolded, species that are on-pathway both in refolding and in unfolding.

A unique protein fold, the α-helical Greek key, is found only in the death domain (DD)[1] superfamily. These protein domains are small, generally about 100 amino acids, and consist of six α-helices folded into a Greek key topology. The members of the DD superfamily play specific roles in apoptosis, the inflammatory response, or transcriptional activation.

The DD superfamily includes members containing the death domain, the death effector domain (DED), the pyrin domain, and the caspase recruitment domain (CARD) (*1*−*3*). The CARD-containing protein family includes many biologically important proteins that play key roles in essential mechanisms for cell survival or cell death (*4*, *5*). The biological function of the CARD domain is to convey cellular signals, and this is accomplished through hetero- or homo-oligomerizations that allow the domains to function as bridging proteins to larger protein complexes (*1*, *3*, *6*, *7*). The CARD−CARD interactions are highly specific (*4*). While hydrophobic interactions are considered the primary driving force for the interactions, electrostatic contacts between surface patches of the CARDs determine the binding specificity (*8*).

A novel serine/threonine kinase, RICK (CARDIAK, RIP2) (RIP-like interacting CLARP kinase), is a CARD-containing protein found in the cytosol (*9*, *10*). RICK is expressed in multiple human tissues and regulates several cellular mechanisms: apoptosis initiated by CD95 (also called Fas) through enhancement of caspase-8 activation, activation of JNK (Jun N-terminal kinase) and NF-κB, and initiation of inflammatory responses by activating procaspase-1 (*9*−*11*). It was shown that RICK mediates signal transduction responses for both innate and adaptive immune systems and is a key therapeutic target for bacterial-induced inflammation (*12*, *13*). RICK contains an N-terminal serine/threonine kinase catalytic domain and a C-terminal CARD. Both the catalytic domain and the CARD are required for CD-95 mediated apoptosis and NF-κB activation (*9*, *10*), although only the CARD domain is required for the activation of procaspase-1 (*11*).

While the amino acid sequence identities of CARDs are quite low (<20%), the structures of several family members are known and demonstrate the structural homology within the family (*14*−*21*). All CARD structures show the same topology, the α-helical Greek key, and nearly identical tertiary structures, with minor variations (*1*). These protein domains are comprised of six antiparallel α-helices that tightly surround a hydrophobic core, with many charged residues on the surface. The arrangement of the helices results in a Greek key topology (Figure 1A), in contrast to most helical bundles in which sequential helices pack adjacently in antiparallel directions.

The folding of several small helical bundles, such as cytochrome *c* (*22*, *23*), acyl-CoA binding protein (*24*, *25*), λ-repressor (*26*, *27*), and immunity proteins (*28*−*32*), has been studied. In general, their folding rates are fast (from ∼300 to ∼5000 s^{-1}) (*33*, *34*) and can be predicted by their contact order, an algorithm based on the average sequence

* To whom correspondence should be addressed at the Department of Molecular and Structural Biochemistry, 128 Polk Hall, North Carolina State University, Raleigh, NC 27695-7622. Phone: (919) 515−5805. Fax: (919) 515−2047. E-mail: clay_clark@ncsu.edu.

[1] Abbreviations: CARD, caspase recruitment domain; RICK, RIP-like interacting CLARP kinase; RICK-CARD, CARD of RICK; DD, death domain; DED, death effector domain; APAF-1, apoptotic protease activating factor; IPTG, isopropyl β-D-1-thiogalactopyranoside. Standard abbreviations are used for the amino acids.

10.1021/bi0340752 CCC: $25.00
Published on Web 05/01/2003

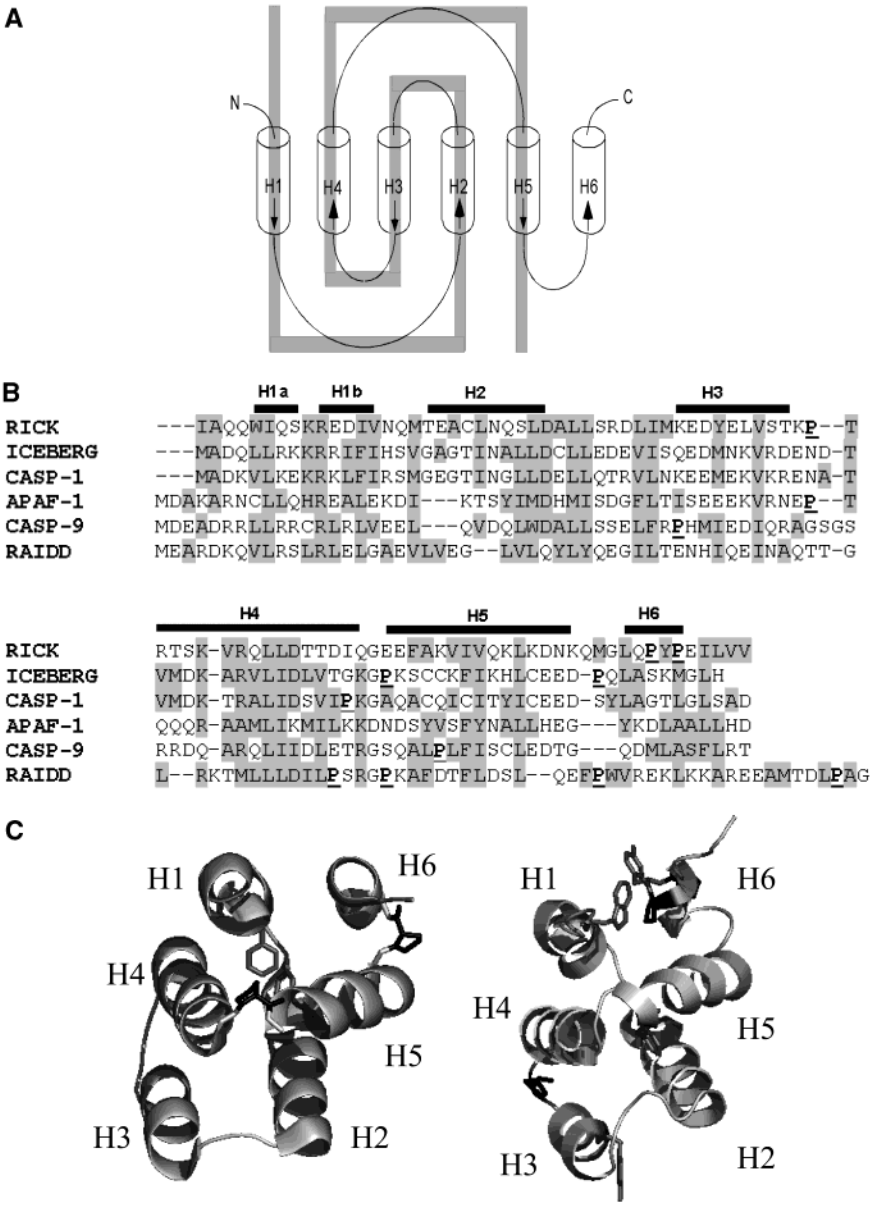

FIGURE 1: (A) Folding topology of α-helical Greek key of the DD superfamily (ref *15*). The helices are represented as cylinders with orientation indicated by the arrows. The N- and C-termini are indicated as well. (B) Sequence alignment of CARDs. The helical regions of ICEBERG are indicated above the alignment. The CARDs of RICK, ICEBERG, procaspase-1 (CASP-1), APAF-1, procaspase-9 (CASP-9), and RAIDD are listed. The homologous regions are highlighted in gray. Proline residues are underlined and in bold. (C) The structure of ICEBERG (left) and the homology model of RICK-CARD (right). Structures were drawn with Pymol (DeLano scientific, CA). ICEBERG (PDB code 1DGN) is shown in ribbon diagram with the proline residues in black and the aromatic residues, two phenylalanines, in gray. The homology model of RICK-CARD in ribbon diagram was generated by Insight II using ICEBERG (PDB code 1DGN) as the template. The sequence alignment for modeling is shown in Panel B. The three prolines are colored in black. The aromatic residues, one tryptophan in helix 1, two tyrosines in helix 3 and 6, and one phenylalanine in helix 5, are in gray.

distance between all pairs of contacting residues in the native structure (*35*, *36*). Also, there are a few β-Greek key proteins, comprised of β-strands in the Greek key topology, which have been examined, such as immunoglobulin-like superoxide dismutase (*37*−*39*), $\beta\gamma$-crystallin (*40*, *41*), fibronectin type III domain (*42*), and azurin (*43*−*45*). While the mechanisms of folding are not known for the complex Greek key topology, two nucleation models have been suggested. The β-hairpin model suggests that folding occurs initially through a long β-hairpin, and then the protein folds up two strands at a time (*46*, *47*). Alternatively, the β-zipper model suggests that a hydrophobic core forms initially via two adjacent strands connected by a short loop (*48*). In addition, a highly conserved tyrosine in the "tyrosine corner" motif of the β-Greek key proteins was shown to be important to the stability and the early structure formation of fibronectin type III domain (*42*) and to the equilibrium folding of pseudoazurin (*42*, *49*). However, such a motif is not found in the α-Greek key proteins.

Because of these considerations, we examined the equilibrium and kinetic folding of RICK-CARD. We show that RICK-CARD is a marginally stable protein, and an apparent two-state folding process can describe the equilibrium folding/unfolding. The protein stability decreases somewhat in moderate salt concentrations but increases in high salt concentrations, suggesting that surface charge repulsions do not decrease the protein stability in the absence of salts, as observed in other small proteins (*50*−*52*). The time course

of refolding and of unfolding were examined by single mixing, double jump and interrupted refolding stopped-flow techniques. The results show that both the unfolding and refolding reactions are complex and contain multiple phases. Overall, the data suggest the presence of several partially folded, intermediate, conformations and that the intermediates are obligatory and on-pathway.

MATERIAL AND METHODS

Reagents. Ultrapure urea was purchased from Nacalai Tesque Inc. (Kyoto, Japan). Dithiothreitol (DTT) was either from Sigma or Denvil. Trizma-Base (Tris), sodium chloride (NaCl), potassium chloride (KCl), monobasic and dibasic potassium phosphate (KH_2PO_4, K_2HPO_4), sodium sulfate (Na_2SO_4), isopropyl β-D-1-thiogalactopyranoside (IPTG), ethylenediaminetetraacetic acid (EDTA), DEAE sepharose, ampicillin, antifoam-C, and DNase I were from Sigma. All buffers were filtered through either 0.45 or 0.22 μm filter membranes. The urea-containing buffers were prepared as described previously (*53*).

Plasmid Construction. The cDNA encoding the CARD domain of RICK was obtained from PCR amplification using the template pcDNA3-RICK (*10*) (kindly provided by Dr. Gabriel Núñez, University of Michigan). The forward and reverse primers used for PCR amplification were 5′-GTCTGCAGCATATGATAGCCCAG-3′ and 5′-GTAAATT-TAACTCGAGTCATCTAGAAACC-3′, respectively. The PCR product was subcloned into pET21a (Novagen) using the restriction enzymes *Nde*I and *Xho*I. The resulting plasmid was named pCARD-RICK. The resulting protein, CARD of RICK (RICK-CARD), is composed of 95 amino acids, from isoleucine 426 to arginine 519 of RICK. In this construct, an N-terminal methionine was generated by the cloning procedure. The calculated molecular mass of RICK-CARD is 10 917 Da.

Protein Purification. *E. coli* BL21 (DE3) cells were transformed with pCARD-RICK. Cells were grown in Fernbach flasks containing 1 L of LB media, ampicillin (50 μg/mL) and antifoam-C (0.003%) at 37 °C and 300 rpm. When the A_{600} of the culture reached 1.2, IPTG was added to a final concentration of 0.4 mM to induce protein expression. The culture was harvested 4 h after induction by centrifugation for 20 min at 5000 rpm (GS3 rotor, Sorvall) and 4 °C. The cells were resuspended in about 15 mL of lysis buffer (30 mM Tris-HCl, pH 8, 1 mM DTT, and 1 mM EDTA) per 1 L of culture, and were broken by French Press at 16 000 psi followed by centrifugation for 30 min at 14 000 rpm (SA-600 rotor, Sorvall) to separate the soluble and insoluble portions. The pellet was resuspended and washed for 1 h at room temperature by stirring the pellet in buffer A (30 mM Tris-HCl, pH 8, and 1 mM DTT) containing 50 mM $MgCl_2$ and 0.1 mg of DNase I/100 mL of lysate. After the wash, the solution was centrifuged at 14 000 rpm for 30 min at 4 °C. The pellet was dissolved in 5 mL of buffer A containing 8−9 M urea/1 L culture, and was incubated on ice for 1 h. The solution was then centrifuged for 30 min at 14 000 rpm and 4 °C to remove cell debris. The solubilized protein was rapidly diluted into ice-cold buffer A containing 0.1 M NaCl, and the solution was incubated for 15 min. The final protein concentration for refolding was approximately 0.05 mg/mL based on estimation by A_{280}. The refolded protein was concentrated to approximately 50 mL and centrifuged for 30 min at 14 000 rpm. The supernatant was dialyzed against buffer A (4 °C).

RICK-CARD eluted from a DEAE-sepharose column (2.6 × 25 cm, Sigma) equilibrated with buffer A at 4 °C using the following procedure. The protein was loaded onto the column, and the column was washed with 200 mL of buffer A. A two-step gradient procedure was used to elute the protein. First, a linear gradient of buffer A containing 0 to 300 mM NaCl, with a total volume of 500 mL, was used. This was followed by a linear gradient of buffer A containing 300 to 500 mM NaCl, with a total volume of 500 mL. The flow rate was 4 mL/min. RICK-CARD eluted between 200 and 250 mM NaCl. The fractions were analyzed by 4−25% SDS−PAGE. The pure protein fractions were pooled, concentrated, and dialyzed against buffer A. The extinction coefficient at 280 nm of RICK-CARD was calculated (*54*) to be 8250 M^{-1} cm^{-1}.

Molecular Modeling. The homology model of RICK-CARD was generated using the homology module of Insight II (Molecular Simulation Inc.). The sequences of the CARDs were aligned based on the conserved residues, hydrophobic core residues, and the secondary structural elements, and the alignment used to generate the structural model is shown in Figure 1B. The NMR structure of ICEBERG, another CARD-containing protein (*18*), was used as the modeling template (from Protein Data Bank, accession number 1DGN). The sequence identity of ICEBERG and RICK-CARD is 21%.

Fluorescence and Circular Dichroism (CD) Spectroscopy. Fluorescence emission spectra were obtained with a PTI C-61 spectrofluorometer (Photon Technology International). RICK-CARD (3 μM) was excited at 280 or 295 nm, and the emission spectra were measured from 300 to 400 nm. CD spectra were obtained with a J600A spectropolarimeter (Jasco Inc.). The protein concentrations for both far- and near-UV CD were 57 μM, and the samples were in buffer B (10 mM Tris-HCl, pH 8, 1 mM DTT). The path length of the CD cells used was 0.1 cm (far-UV) or 1 cm (near-UV). All spectra were corrected for buffer signals. The experiments were done at 25 °C, and the temperature was held constant using a circulating water bath.

Equilibrium Folding/Unfolding. Stock solutions of native RICK-CARD were prepared in buffer A for fluorescence measurements and in the buffer B for CD measurements. Stock solutions of unfolded RICK-CARD were prepared in the same buffers containing 6 M urea. Both stocks (native and unfolded protein) contained the same protein concentration and were incubated at room temperature for at least 30 min prior to the experiments. A titrator (Olis Inc.) was used for equilibrium folding studies by fluorescence emission, and an incubation time of 1500 s was used after each injection. It was determined that this time is sufficient to allow for equilibration. Samples were excited at 280 or 295 nm, and fluorescence emission was monitored from 300 to 400 nm.

The emission spectra at each urea concentration were examined as described previously (*55*) to determine the average emission wavelength, $\langle\lambda\rangle$, using eq 1,

$$\langle\lambda\rangle = \sum_{i=1}^{N}(I_i\lambda_i)/\sum_{i=1}^{N}(I_i) \qquad (1)$$

where I_i is the fluorescence emission signal at wavelength λ_i. The normalized average emission wavelength was plotted versus urea concentration. The data were fit to a two-state equilibrium process (N ⇆ U) described by Santoro and Bolen (*56*). For the CD experiments, titrations were performed manually by mixing unfolded protein with the native protein. A quartz cuvette with 1-cm path length was used in these experiments. The signal at 220 nm was measured for 120 s, and the data were averaged and corrected for background signals.

Stopped-Flow Fluorescence Studies. The kinetic folding/unfolding experiments were performed using a stopped-flow spectrofluorometer (SX.18MV, Applied Photophysics, UK). The temperature was controlled at 25 °C using a circulating water bath. The samples were excited at 280 nm and the fluorescence emission was measured using a cutoff filter of 305 nm. The refolding experiments were done by mixing stock protein solutions (33 μM) that had been prepared in buffer A-containing 4 M urea (unfolded protein) with buffer A. The final protein concentration was 3 μM, and a mixing ratio of 1:10 was used. Stock protein (33 μM) in 4 M urea-containing buffer was mixed with buffer A-containing urea between 0 and 4 M, as shown in the figures. For unfolding experiments, stock protein (33 μM) in buffer A was mixed with buffer A-containing urea between 0 and 4 M. The final protein concentration was 3 μM, and a mixing ratio of 1:10 was used. The final urea concentrations are shown in the figures.

Double Jump and Interrupted Refolding Stopped-Flow Experiments. The experiments were performed with a stopped-flow spectrofluorometer (SX.18MV, Applied Photophysics, UK) using the sequential mixing mode. The temperature was held constant at 25 °C. In general, the first jump was performed with a mixing ratio of 1:1 using two buffer solutions, described below. After a specified delay time, the solution from the first jump was rapidly mixed with a third solution using a mixing ratio of 1:5. Incubation (delay) times from 0.1 to 900 s were used after the first jump.

For double jump experiments (*57*), native RICK-CARD (36 μM) in buffer A was mixed with buffer A-containing 8 M urea for the first jump. After various delay times, as described in the text, the protein solution was mixed with buffer A for the second jump. The signal trace was monitored for 200 s. The final protein concentration was 3 μM, and the final urea concentration was 0.67 M. The native protein signal was determined from the final signal of the experiment that used a 900 s delay time. To obtain the signal of the unfolded protein, the third solution, described above, was changed to buffer A-containing 4 M urea.

For interrupted refolding experiments (*58*, *59*), unfolded RICK-CARD (36 μM) in buffer A-containing 3 M urea was mixed with buffer A for the first jump. After various delay times, as shown in the figures, the protein solution was mixed with buffer A-containing 4 M urea. The final urea concentration was 3.58 M, and the final protein concentration was 3 μM. The signal for the unfolded protein was obtained from the final signal of the experiment that used a 900 s delay time. To obtain the signal of the native protein, the third solution was changed to buffer A-containing 1.5 M urea.

RESULTS

General Properties of RICK-CARD. The CARD of RICK (called RICK-CARD) used in these studies is a 95-amino acid protein that contains six α-helices arranged in a Greek key topology (Figure 1A). With a few exceptions, the amino acid sequence identities of the CARD family members are less than 20% (see also Figure 1B) (*1*, *60*, *61*), although structural data for several CARDs demonstrate that the Greek key topology is conserved (*14*−*21*). While the structure of RICK-CARD has not been determined, we generated a homology model using the solution structure of ICEBERG (*18*) as the template and the sequence alignment shown in Figure 1B. The results of the model are shown in Figure 1C, where the model of RICK-CARD is compared to the structure of ICEBERG. The model of RICK-CARD shows a well-packed core of hydrophobic residues with exposed charged residues. The least defined region of the RICK-CARD model is helix 6, but as described below, this is true of other CARD proteins as well. RICK-CARD contains one tryptophan, which is located in helix 1, and two tyrosines, which are located in helices 3 and 6. A single phenylalanine is located in helix 5. There are no disulfide bonds or prosthetic groups.

Fluorescence emission spectra of RICK-CARD, using intrinsic fluorescence probes, are shown in Figure 2A. When the native protein is excited at 295 nm, which excites only the tryptophanyl residue, the emission maximum is 330 nm, demonstrating that the tryptophanyl residue is relatively buried. The spectrum shifted to 350 nm when the protein was unfolded in urea-containing buffer, demonstrating that the tryptophanyl residue is exposed under these conditions. In addition to fluorescence emission, we examined the secondary and tertiary structures of RICK-CARD using near- and far-UV circular dichroism. The far-UV CD spectrum (Figure 2B) shows double minima at 206 and 218 nm, similar to that of other CARDs (*2*). The near-UV CD spectrum (Figure 2C) shows a minimum at 278 nm. Both signals decreased when the protein was incubated in urea-containing buffer. Overall, the data show that the protein is folded with a well-packed tertiary structure. In 4 M urea-containing buffer, the spectra are consistent with those of unfolded proteins.

Equilibrium Folding of RICK-CARD. The equilibrium folding/unfolding of RICK-CARD was examined by monitoring the changes in fluorescence emission upon incubation in urea-containing buffer. The samples were excited either at 280 nm, to excite all aromatic residues, or 295 nm, to excite the single tryptophanyl residue. In addition, the changes in CD at 220 nm were determined. Representative data are shown in Figure 3. The results show that the three spectroscopic probes overlay, suggesting that the loss of secondary structure is concomitant with the loss of tertiary structure. The experiments were repeated over a range of protein concentrations (1.5−12 μM) and did not vary from those shown in Figure 3 (data not shown). While some CARDs have been shown to form homooligomers at higher protein concentrations, RICK-CARD is a monomer under the experimental conditions described here (30 mM Tris-HCl, pH 8, 1 mM DTT, 25 °C, 12 μM or less protein).

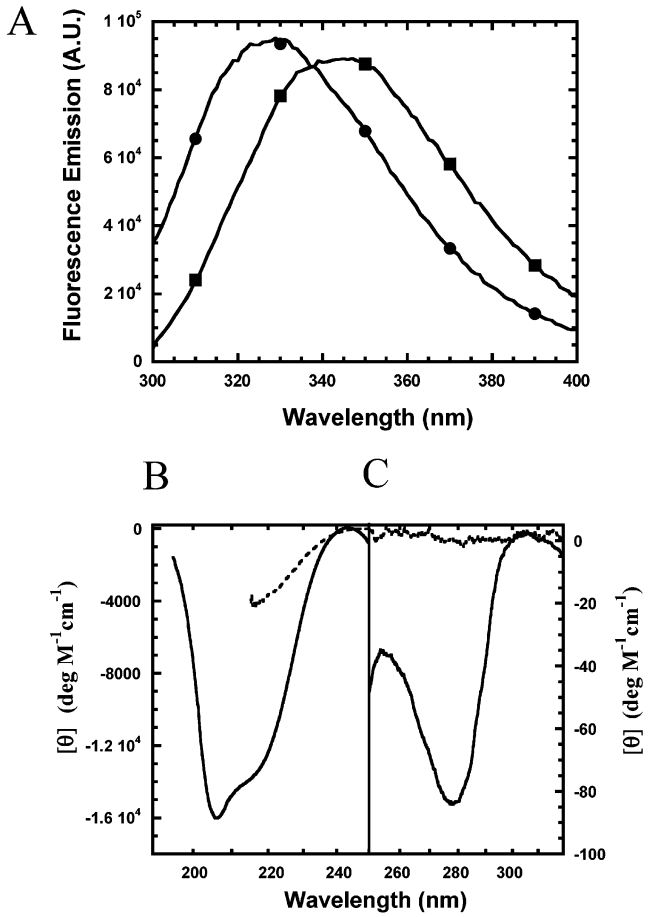

FIGURE 2: (A) Fluorescence emission spectra of RICK-CARD. The protein (3 μM) in buffer (●) or in 3 M urea-containing buffer (■) was excited at 295 nm. The fluorescence emission was collected from 300 to 400 nm. (B) Far-UV and (C) near-UV CD spectra of RICK-CARD. The spectra of native protein in buffer (solid line) and the denatured protein in 4 M urea-containing buffer (dash line) are shown.

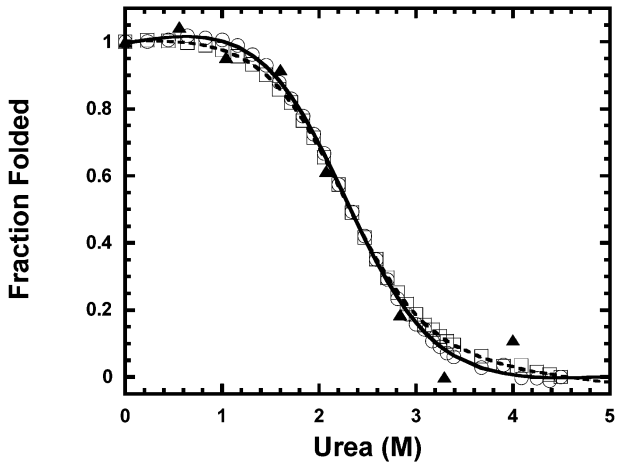

FIGURE 3: Equilibrium unfolding of RICK-CARD. The average emission wavelength was determined for fluorescence emission spectra as described in methods. The normalized average emission wavelength and CD data versus urea concentrations are plotted. The fluorescence emission data from excitation at 280 (○), or 295 nm (□) of RICK-CARD (3 μM) as well as the CD data at 220 nm (▲) of RICK-CARD (6 μM) are shown. The solid line and dashed line represent fits of the data from excitation at 280 and 295 nm, respectively, to a two-state equilibrium folding mechanism. The ΔG^{H_2O} and *m*-value obtained for excitation at 280 nm are 2.9 kcal/mol and 1.3 kcal mol^{-1} M^{-1}, respectively. The ΔG^{H_2O} and *m*-value for excitation at 295 nm are 3.1 kcal/mol and 1.4 kcal mol^{-1} M^{-1}, respectively, at 25 °C.

The results shown in Figure 3 are well-described by a two-state equilibrium folding model, representing only the native and unfolded states of the protein. The conformational free energy, ΔG^{H_2O}, and the cooperativity index, *m*, determined from fits of the data to the two-state equilibrium model are 3.0 ± 0.15 kcal/mol and 1.27 ± 0.06 kcal mol^{-1} M^{-1}, respectively. The *m*-value is thought to represent the change in surface area of the protein exposed to solvent upon unfolding (*62*, *63*). Scholtz and co-workers (*64*) have described a qualitative correlation between the *m*-value and the change in the solvent exposed surface area (ΔASA). Using their equations, we calculate the ΔASA of RICK-CARD to be 8200 Å^2, corresponding to 98 residues. This is in excellent agreement with the number of amino acids of RICK-CARD, 95.

Influence of Salts on Protein Stability. Long-range electrostatic interactions on the surface of several small proteins (*50*, *52*, *65*) have been shown to affect the conformational free energy. In some cases, charge repulsions on the protein surface have been shown to destabilize the native conformation of the protein (*50*, *52*, *65*). In addition, CARD−CARD interactions are known to be influenced by the charged groups on the protein surface (*8*). The calculated pI of RICK-CARD is 5.3, although it contains 13 basic and 14 acidic residues, and the charge of the protein at pH 8, the conditions of the equilibrium unfolding experiments, is about −1.5. Because of these considerations, we examined the effects of various salts on the protein stability.

The urea unfolding studies were done in buffers containing NaCl, KCl, KH_2PO_4/K_2HPO_4, or Na_2SO_4. Representative data for the experiments in which NaCl was included in the buffers are shown in Figure 4A. Overall, the unfolding profiles were similar over the entire range of salt, although the amount of urea required to unfold the protein increased between 200 mM and 2 M NaCl. Similar results were obtained for experiments in which the other salts were examined (data not shown), with the exceptions noted below. The data were well-described by a two-state equilibrium model, and the results of the fits are summarized in Figure 4B. The *m*-value did not change significantly in the presence of salt, indicating that equilibrium folding intermediates are not stabilized under these conditions. At low concentrations of NaCl or KCl, between 0 and 200 mM, the midpoint, or $urea_{1/2}$, decreased from 2.4 to ∼1.8 M urea, and the ΔG^{H_2O} decreased from 3.0 to 2.5 kcal/mol. These results suggest that in RICK-CARD electrostatic interactions are stabilizing, and the favorable Coulombic interactions are screened at low ionic strength. Alternatively, Lee et al. (*66*) have shown that at ionic strengths near physiological values, pairwise Coulombic interactions are weak at distances greater than 5 Å, but in aggregate, the long-range interactions can affect the properties of the protein. For example, long-range, repulsive, interactions can have a significant effect if not balanced by favorable interactions. Thus, it is possible that for RICK-CARD unfavorable Coulombic interactions become more important at low ionic strength. Above 200 mM salt, the $urea_{1/2}$ increased so that at 2 M NaCl, ΔG^{H_2O} was 7.3 kcal/mol. These results are consistent with Hofmeister effects (*67*, *68*). Similar results have been described for the cold shock

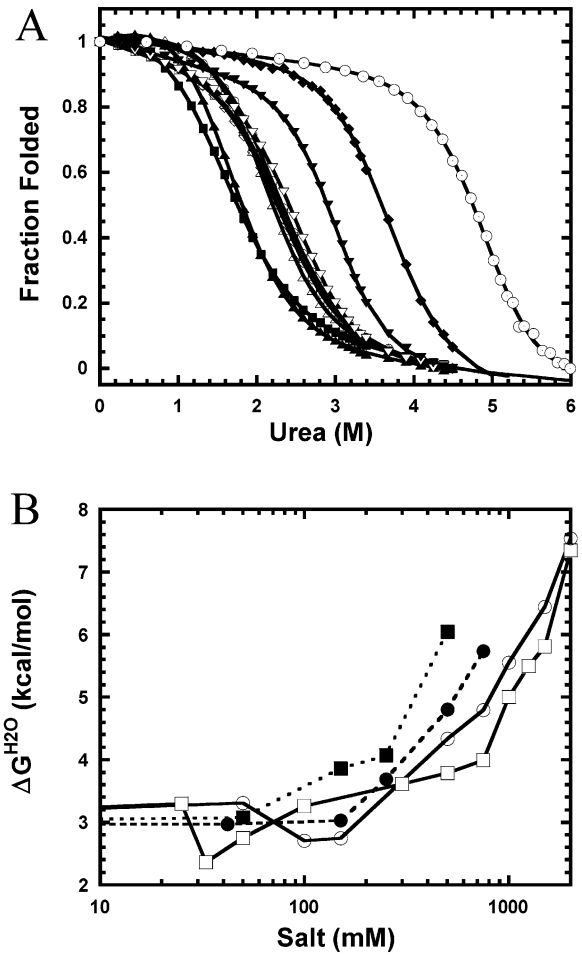

FIGURE 4: (A) Equilibrium unfolding of RICK-CARD in the presence of NaCl. NaCl concentration ranges from 0 to 2 M is indicated: 0 (○), 33 (■), 50 (▲), 100 (△), 300 (◇), 500 (□), 750 (▽), 1000 (▼), 1500 (◆), 2000 (⊙) mM. The solid lines are fits to a two-state equilibrium mechanism, and the results are shown in Panel B. (B) Conformational free energy versus salt concentration. The ΔG^{H_2O} was obtained from the fits of the equilibrium unfolding of RICK-CARD (3 μM) in the presence of four salts: NaCl (□), KCl (○), KH_2PO_4/K_2HPO_4 (●), and Na_2SO_4 (■). The solid lines are not fits but are present as a guide.

protein (Csp) from the thermophilic organism *Bacillus caldolyticus* (*51*, *65*). As expected for electrostatic interactions that are screened by counterions, the divalent ions were more effective than the monovalent ions, and the effects are shifted to lower salt concentrations. The data show that the response is not cation or anion dependent and probably precludes the binding of ions to specific sites on the protein.

Folding Kinetics of RICK-CARD. The time courses of refolding and of unfolding RICK-CARD were examined in single-mixing stopped-flow experiments by monitoring changes in fluorescence emission. The data are shown in Figure 5A, and several kinetic phases are observed in both experiments. First, a burst phase is present in both the unfolding and refolding profiles. In unfolding, the burst phase accounts for approximately 55% of the total signal change, whereas in refolding the burst phase accounts for approximately 65% of the total signal change. Second, following the burst phase the unfolding data are fit best to a three exponential process in which the three phases have similar amplitudes. The refolding data also are fit best to a three exponential process. Residuals for fits of the refolding data to two or three exponential processes are shown in Figure 5B. The results demonstrate that although the amplitude of the middle phase is small, the data are fit better to a three-exponential process.

For refolding, the apparent rate constant of the fast phase is 21 s^{-1}, whereas those of the intermediate and slow phases are 1 and 0.012 s^{-1}, respectively. The intermediate phase accounts for only ∼3% of the refolding signal change, whereas those of the fast and slow phases account for ∼54 and ∼43%, respectively. For unfolding in 4 M urea-containing buffer, the apparent rate constant of the fast phase is ∼1 s^{-1}, whereas those of the intermediate and slow phases are 0.08 and 0.014 s^{-1}, respectively. Each phase accounts for about 15% of the total signal change. Overall, the results demonstrate that there are at least four phases in unfolding and in refolding: a burst phase within the instrumental dead time, a fast phase, with a half-time of ∼50 ms (refolding) or ∼0.5 s (unfolding), an intermediate phase with a half-time of ∼1 s (refolding) or ∼10 s (unfolding) and a slow phase, with a half-time of ∼50 s.

To examine whether the burst phases represent the formation of transient intermediates, we performed the experiments in several final urea concentrations, from 0 to 4 M. The results are shown in Figure 5C. For refolding, the data show that there is a linear decrease of the initial signal from 4 to 0.5 M urea. This demonstrates that the burst phase in refolding does not correlate with the formation of a transiently populated partially folded, or intermediate, conformation. In contrast, the change in the burst phase amplitude is cooperative in the unfolding experiments. The data show that the burst phase in unfolding does correlate with formation of a transiently populated intermediate, and in 4 M urea-containing buffer, the burst phase amplitude accounts for approximately 55% of the total signal change. The burst phase amplitudes for unfolding were fit to a two-state equilibrium unfolding model, and the ΔG^{H_2O} and *m*-value determined from the fits are 2 kcal/mol and 0.93 kcal mol^{-1} M^{-1}, respectively. These values account for about 70% of the total ΔG^{H_2O} and *m* determined from equilibrium unfolding (Figure 3).

As shown in Figure 5C, the final signal (at ∼100 s) accounts for the total change in signal between native and unfolded protein. The final amplitudes were fit to a two-state equilibrium model, and the ΔG^{H_2O} and *m*-value determined from the fits are 2.6 kcal/mol and 1.3 kcal mol^{-1} M^{-1}, respectively. These values are in good agreement with those determined from the equilibrium unfolding experiments (Figure 3). As shown in Figure 5D, the final signals of unfolding and refolding superimpose to the equilibrium unfolding data, demonstrating that the final conditions of the kinetic experiments are equivalent to those at equilibrium.

In addition to the burst phases, there are three other phases in the refolding and unfolding profiles. The apparent rate constants of the phases were determined in several final urea concentrations, from 0 to 4 M, and the results are shown in Figure 5E. For the fast phases, the apparent rate constant, k_{obs}, generates a chevron plot, where the midpoint of the curve is approximately 2.7 M urea, similar to the midpoint determined from the equilibrium unfolding data (2.4 M urea). For the intermediate phase of refolding, k_{obs} decreased with urea such that at concentrations >1.5 M, the refolding data

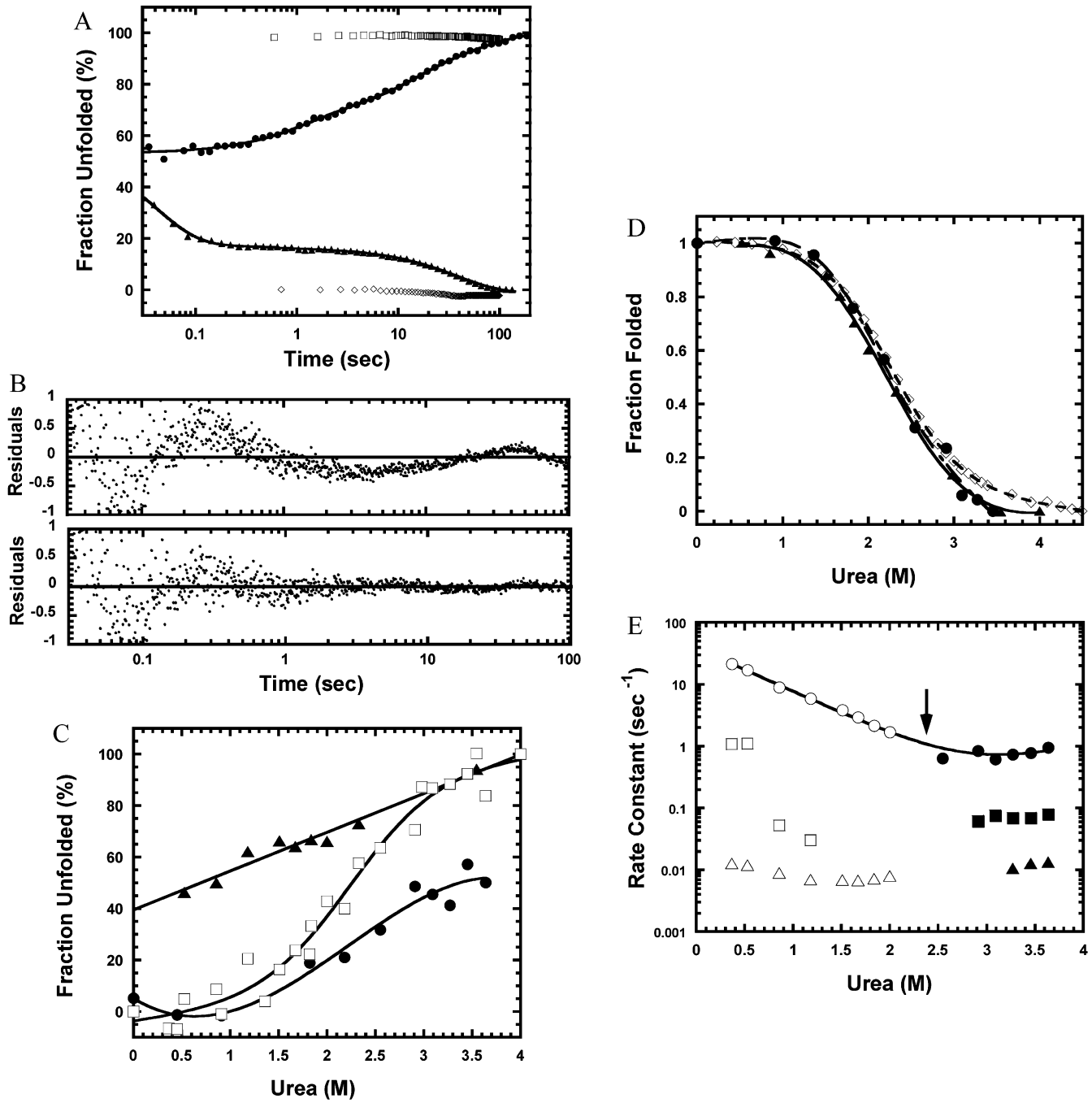

FIGURE 5: The unfolding and refolding kinetics of RICK-CARD. (A) The refolding and unfolding signals versus time. The native (◇) and unfolded protein signals (□) are indicated. Both unfolding (●) and refolding traces (▲) are shown. Solid lines represent fits of the unfolding and refolding traces to a three exponential equation. Parameters obtained from the fits are given in the text. (B) Residuals of fits of the refolding data (▲) shown in panel A. The upper and lower panels are the residuals of two or three exponential fits, respectively. (C) Burst phase signal of the refolding and unfolding reactions versus urea concentration. The initial signal of refolding (▲), the initial signal of unfolding (●), the final signal (□) from both studies, and the fits (solid lines) are plotted. The initial signals of refolding were fit to a linear equation. The initial signals of unfolding were fit to a two-state folding mechanism where the ΔG^{H_2O} is 2.0 kcal/mol and the *m*-value is 0.93 kcal mol^{-1} M^{-1}. The final signals from both studies were fit to a two-state folding mechanism where the ΔG^{H_2O} is 2.8 kcal/mol and the *m*-value is 1.26 kcal mol^{-1} M^{-1}. (D) The final signals of refolding (▲) and unfolding (●) versus urea concentrations. Both final signals are superimposed to the equilibrium folding experiment (◇). The lines are fits to a two-state folding mechanism. (E) The observed rate constants (k_{obs}) for unfolding and for refolding versus urea concentration. The k_{obs} is determined from the three-exponential fit from the unfolding (closed symbols) and refolding kinetics (open symbols). The midpoint from the equilibrium unfolding studies (Figure 3) is indicated (2.4 M urea). The solid line represents a fit to eq 2. Parameters obtained from the fits are given in text.

were equally well fit to a two-exponential process. For the intermediate phase of unfolding as well as the slow phases, k_{obs} did not vary over 2-fold, suggesting that those rates were independent of the final urea concentration.

The data for the fast phases were fit to a two-state kinetic mechanism using eq 2 (*28*, *69*)

$$k_{obs} = k_{UN} \exp(-m_{U-TS}[\text{urea}]/RT) + k_{NU} \exp(m_{N-TS}[\text{urea}]/RT) \quad (2)$$

where k_{obs} is the observed rate constant of the fast phase, k_{UN} and k_{NU} are the rate constants of refolding and of unfolding, respectively, in the absence of denaturant, and

m_{U-TS} and m_{N-TS} reflect the change in solvent accessible surface area between the unfolded and native states, respectively, relative to the transition state ensemble. Values of 32 and 0.13 s^{-1} were obtained for k_{UN} and k_{NU}, respectively, and values of 0.90 and 0.37 kcal mol^{-1} M^{-1} were obtained for m_{U-TS} and m_{N-TS}, respectively.

The Gibbs free energy and *m*-value between the native and unfolded states of RICK-CARD can be calculated from the kinetic experiments using eqs 3 and 4, respectively (*28*, *69*).

$$\Delta G^{H_2O} = -RT \ln(k_{NU}/k_{UN}) \quad (3)$$

$$m_{UN} = m_{U-TS} + m_{N-TS} \quad (4)$$

The calculations show that the Gibbs free energy of RICK-CARD is 3.3 kcal/mol, and the *m*-value is 1.26 kcal mol^{-1} M^{-1}. These values are in good agreement with those described for the equilibrium unfolding studies (Figure 3), where the ΔG^{H_2O} is 3.0 ± 0.15 kcal/mol and the *m*-value is 1.27 ± 0.06 kcal mol^{-1} M^{-1}. Using eq 5, we calculated the

$$\beta^{\ddagger} = m_{U-TS}/m_{UN} \quad (5)$$

$\beta^{\ddagger}$ value of RICK-CARD to be 0.71. As described by Chen and co-workers (*70*), the $\beta^{\ddagger}$ value describes the compactness of the transition state ensemble relative to that of the native state ($\beta^{\ddagger} = 1$) and of the unfolded state ($\beta^{\ddagger} = 0$) ensembles and refers to the position of the transition state on a folding reaction coordinate. The data presented here demonstrate that the transition state ensemble of RICK-CARD is compact, which indicates that many native-state contacts have formed in this folding reaction.

Double Jump Stopped-Flow Studies. Sequential mixing, or double jump, experiments were performed to investigate further the slow phases observed in the folding reactions of RICK-CARD. In the first jump, the native protein was mixed with urea-containing buffer so that the final urea concentration was 4 M. As shown in Figure 3, this urea concentration is sufficient to unfold the protein. During the first jump the time in which the protein was incubated in urea was varied from 0.1 to 900 s. In the second jump, the protein was returned to native conditions, and refolding was monitored. This procedure allows one to examine slow equilibration processes in the unfolded protein and has been used to examine the isomerization of prolyl (Xaa−Pro) peptide bonds (*71*, *72*). The homology model of RICK-CARD (Figure 1C) suggests that the three prolyl residues are found in the trans configuration in the native protein. However, due to the low sequence identity of CARD proteins (Figure 1B), the isomeric states of the prolines are not well determined in our structural model. If one of the three prolines resides in the cis isomer, then the unfolded state ensemble would consist of (1/6) × $(5/6)^2$ or 11.6% of molecules in their native isomer at equilibrium, if one assumes a cis/trans ratio of 1:5 (*43*, *73*). If two prolyl residues reside in the cis isomer, then the unfolded state ensemble would consist of 2.3% of molecules in their native isomer at equilibrium. Thus, Xaa−Pro bonds in the cis configuration can have significant effects on the population of native isomers in the unfolded state ensemble. Assuming a three state model ($N \leftrightarrows U_f \leftrightarrows U_s$) holds for RICK-CARD, in which N refers to the native protein, and U_f and U_s refer to the unfolded protein in the native or non-native isomer, respectively, the double jump experiment should reflect the population of molecules with the native isomeric state prior to prolyl isomerization.

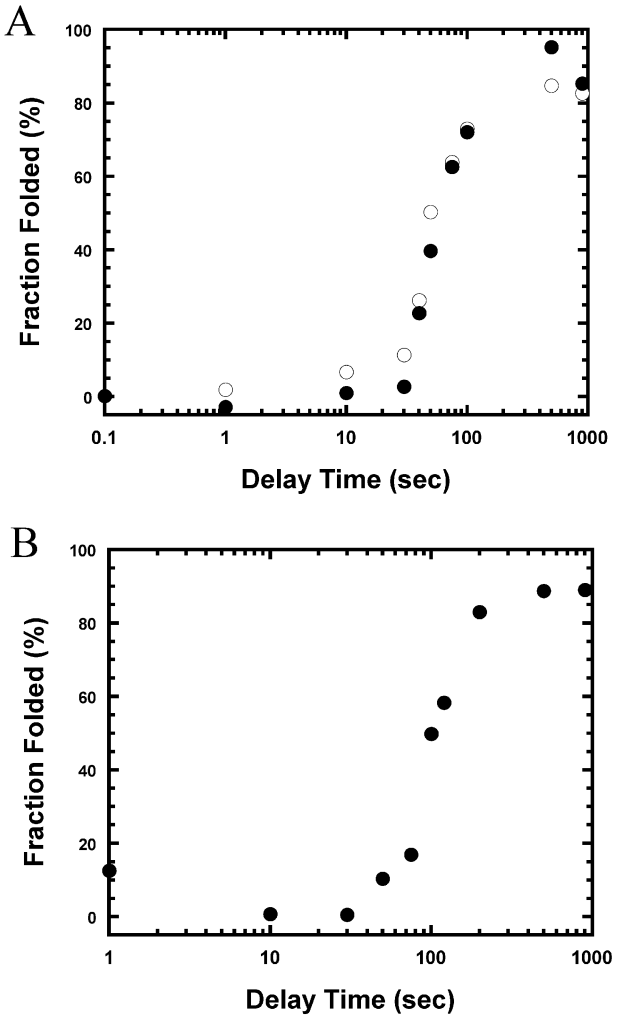

FIGURE 6: (A) Fraction of native protein versus delay time in double jump experiments. The initial (○) and final signals (●) of the signal traces were normalized to fraction folded and plotted versus delay time. (B) Fraction of native protein versus delay time in interrupted refolding experiments. The initial signal was normalized and plotted versus delay time.

The results of the double jump experiments for RICK-CARD are shown in Figure 6A. Surprisingly, the short delay times resulted in little or no native protein formation upon refolding. The data show a lag phase of approximately 20 s followed by a second phase in which the population of native protein increases exponentially. At a minimum, the results rule out the sequential model described above. In that mechanism, the non-native isomer develops slowly from the unfolded protein, and the population of native protein decreases with longer delay times. Qualitatively, the two phases observed in the double jump experiment are consistent with the apparent rate constants obtained from the two slow phases of the single mixing unfolding experiment (Figure 5A), 0.08 s^{-1} ($t_{1/2}$ = 8.6 s) and 0.014 s^{-1} ($t_{1/2}$ = 49.3 s), respectively. Overall, the results indicate that the intermediates that form during the unfolding of RICK-CARD represent misfolded, or kinetically trapped, species. That is, when RICK-CARD unfolds for a short time, it is trapped in an unfolded-like intermediate state that cannot refold to the

Scheme 1: A Proposed Pathway for Unfolding of RICK-CARD[a]

$$\mathrm{N} \xrightarrow[\text{(burst)}]{[55\ \%]} \mathrm{I_1} \xrightarrow[(1\ s^{-1})]{[15\ \%]} \mathrm{I_2} \xrightarrow[(0.08\ s^{-1})]{[15\ \%]} \mathrm{I_3} \xrightarrow[(0.014\ s^{-1})]{[15\ \%]} \mathrm{U}$$

[a] The percent change in fluorescence emission associated with each reaction is shown above and the folding rates are shown below the reactions. N and U represent native and denatured states, respectively. I_1, I_2, and I_3 represent the non-native sequential intermediates on the pathway.

native state unless the time for unfolding is prolonged. RICK-CARD is able to refold only after the unfolded species is formed, and this occurs with a half-time of ~50 s.

Interrupted Refolding Experiments. The interrupted refolding experiment is similar to the double jump experiment except that it is employed to examine details of the refolding pathway. In the first jump, the unfolded protein is refolded for various amounts of time, and then it is returned to urea-containing buffer, where unfolding is monitored. The initial signal indicates the amount of native protein formed in various times of refolding, thus the interrupted refolding experiment gives a time course for the formation of native protein. The results for RICK-CARD are shown in Figure 6B. The data demonstrate a lag phase of ~30 s, in which there is little or no formation of native protein. Following the lag phase, a second phase occurs in which the population of native protein increases exponentially. These results provide evidence for the transient population of intermediate, or partially folded, conformations. Only the second phase produces native RICK-CARD. The half-time (~100 s) of the appearance of the native state correlates well with the apparent rate constant for the slow phase in refolding (0.008 s^{-1}, $t_{1/2} = 86$ s in 1.5 M urea, Figure 5E).

DISCUSSION

We have characterized the equilibrium and kinetic folding of a unique protein domain, CARD of RICK, which adopts a α-helical Greek key fold. We have shown that at equilibrium, the folding of RICK-CARD is well described by a two-state mechanism representing the native and unfolded ensembles. The protein is marginally stable, with a ΔG^{H_2O} of 3.0 ± 0.15 kcal/mol and an *m*-value of 1.27 ± 0.06 kcal mol^{-1} M^{-1} (30 mM Tris-HCl, pH 8, 1 mM DTT, 25 °C). While the *m*-value is constant, the protein stability decreases in the presence of moderate salt concentrations (below 200 mM) and then increases at higher salt concentrations. The results are similar to those of the cold shock protein (Csp) from the thermophilic organism *Bacillus caldolyticus* (*51*, *65*) in which it was shown that electrostatic interactions are stabilizing in the native protein. Above 200 mM salt, the results are consistent with Hofmeister effects (*67*, *68*).

The unfolding pathway of RICK-CARD is complex and contains several non-native conformations. For unfolding, the data are consistent with the sequential unfolding model shown in Scheme 1. In this model, the native protein unfolds via three intermediate conformations prior to reaching the unfolded state. The first step in unfolding, N → I_1, is rapid and occurs during the dead time for mixing (~3 ms). The ΔG^{H_2O} and *m*-value, 2 kcal/mol and 0.93 kcal mol^{-1} M^{-1}, respectively, for the burst phase reaction account for about 70% of the total ΔG^{H_2O} and *m* determined from equilibrium unfolding. This suggests that most of the surface area is exposed during this phase of unfolding. Following the burst phase, at least three additional kinetic phases occur, with rate constants of ~1, 0.08, and 0.014 s^{-1}, respectively. The intermediate and slow phases are observed in double jump experiments in which it was shown that the protein must completely unfold (to U in Scheme 1) prior to refolding.

Scheme 2: A Proposed Pathway for Refolding of RICK-CARD[a]

$$\mathrm{U} \xrightarrow[(30\ s^{-1})]{[54\ \%]} \mathrm{I_4} \xrightarrow[(1\ s^{-1})]{[3\ \%]} \mathrm{I_5} \xrightarrow[(0.012\ s^{-1})]{[43\ \%]} \mathrm{N}$$

[a] The percent change in fluorescence emission associated with each reaction is shown above and the folding rates are shown below the reaction. I_4, and I_5 represent the non-native sequential intermediates on the pathway.

The refolding pathway of RICK-CARD also is complex, and the data are consistent with the sequential folding model shown in Scheme 2. In this model, the unfolded protein folds via (at least) two intermediate conformations prior to reaching the native state. The first step (U → I_4) is rapid, with k_{obs} ~ 30 s^{-1} in the absence of denaturant, and accounts for about 54% of the total signal change. The second step (I_4 → I_5) occurs with an apparent rate of 1 s^{-1} and accounts for ~3% of the total signal change. According to Scheme 2, this suggests that the fluorescence properties are similar for I_4 and I_5. This phase is apparent only at low urea concentrations (<1.5 M). The slow phase of refolding (I_5 → N) occurs with an apparent rate of 0.012 s^{-1} and accounts for ~43% of the total signal change. The intermediate and slow phases are observed in the interrupted refolding experiments, where the time course is followed for the appearance of native protein. In that experiment, it was shown that formation of the native conformation occurs only from the slowest phase, consistent with the sequential model shown in Scheme 2.

The data suggest that for unfolding, most of surface area is exposed in first step (N → I_1), where the *m*-value was determined to be 0.93 kcal mol^{-1} M^{-1}. On the basis of the correlation between the *m*-value and the change in the solvent exposed surface area (ΔASA) described by Scholtz and co-workers (*64*), this represents about 66 of the 95 residues in RICK-CARD. The remaining surface area appears to be exposed in the second phase (I_1 → I_2). The data suggest that the intermediates in unfolding are more like the unfolded conformation in that most of the accessible surface area is solvent exposed. For refolding, the data suggest that the fast phase (U → I_4) is the major folding reaction for the protein. This is reflected in the dependence of k_{obs} on urea, demonstrating that most of the surface area is buried in this phase. The data indicate that the intermediates in refolding are more like the native protein in terms of buried surface area rather than the unfolded protein.

Kinetic complexity in unfolding and refolding reactions has been observed for other small proteins (*28*, *43*, *58*, *71*). While the data presented here do not rule out other more complicated off-pathway mechanisms, results from the double jump and interrupted refolding experiments are difficult to reconcile if the intermediates are off-pathway. Overall, the data for RICK-CARD suggest the presence of kinetically trapped, or misfolded, species that are on-pathway both in refolding and in unfolding. At this point, the nature of the species is not clear, but the data suggest that the intermediates are important. Recently, an on-pathway, mis-

folded, kinetically trapped species has been described for apo-pseudoazurin (*43*, *45*). Interestingly, that protein also has a Greek key topology, although it is comprised of β-strands rather than the α-Greek key described for RICK-CARD. In the case of apo-pseudoazurin, folding was shown to be dependent on the isomerization of proline residues from the intermediate conformation. Prolyl isomerization has also been observed in unfolding (*58*, *72*) and may be the source of the slow unfolding reactions described here.

In the case of RICK-CARD, the isomeric states are not well determined for the prolyl residues. The three prolines (P47, in turn 3, and P85 and P87, in helix 6) are predicted to be in the trans configuration based on homology modeling, but the sequence identity is quite low in the CARD family, and this likely affects the reliability of the structural model. Indeed, none of the three prolines is conserved in general (see Figure 1B), although P47 is found also in APAF-1. Prolines are, in some cases, observed in turn 4, between helices 4 and 5, and turn 5, between helices 5 and 6 (*3*). Although in some CARDs (procaspases-4, -5, and -13, for example) single prolines are predicted to be present in helix 6, RICK-CARD and ARC are the only two members of the CARD family with two prolines in helix 6 (*3*). This helix is the least defined region of our structural model, but this is true also for other CARD proteins for which structures have been determined (*8*, *18*). With the exceptions of RAIDD and APAF-1, the amino acid sequences found in helix 6 within the CARD family have low helical propensities. In the case of RICK-CARD, P85 and P87 reside in the middle of the helix. Consequently, the propensity of the amino acid sequence to adopt a helical structure, as predicted by AGADIR (*74*), is lower than any other member of the CARD family. While both prolines are predicted to be in the trans configuration, the PxP motif distorts and disrupts the helix. In other CARDs (*8*, *14*, *15*, *17*, *18*), the docking of helices 1 and 6 is stabilized by hydrophobic contacts from each helix. In the case of RICK−CARD, disrupting helix 6 by insertion of the PxP motif may prevent tight packing of helix 6 with helix 1. Thus, in addition to the cis/trans isomeric states of the prolyl residues, these features may contribute to the kinetic complexity observed in folding and unfolding.

Other sources of kinetic complexity, such as nonprolyl cis peptide bonds, cannot be ruled out. In this regard, at 25 °C, the rate of isomerization, $k_{cis \rightarrow trans}$, for nonprolyl bonds is ∼2.5 s^{-1} (*59*). Although this has been described as an equilibrium process occurring in the unfolded protein, the rate associated with the reaction of $I_4 \rightarrow I_5$ in RICK-CARD (Scheme 2) is consistent with this reaction. However, if one assumes a value of 0.15% for the fraction of cis isomer of nonprolyl peptide bonds (*59*), then about 14% of the polypeptide chains would be predicted to have a cis peptide bond in RICK−CARD. The reaction of $I_4 \rightarrow I_5$ accounts for only ∼3% of the total signal change. If this phase is due to the isomerization of cis/trans nonprolyl peptide bonds, then only a fraction of the peptide bonds are involved in the slow folding reaction.

The presence of intermediates in folding remains controversial (*75*, *76*) as to whether they represent productive, on-pathway species or misfolded, nonproductive off-pathway species. The results presented here suggest that the intermediates in the refolding of RICK-CARD are obligatory and on-pathway. A growing body of evidence for complex folding topologies (*28*, *43*) or larger proteins (>100 amino acids) (*77*, *78*) indicates that the intermediates may limit the search to the native state ensemble.

ACKNOWLEDGMENT

We thank Dr. Stefan Franzen (North Carolina State University) for assistance with the homology modeling and Dr. Gabriel Núñez (University of Michigan) for providing the plasmid pcDNA3-RICK.

REFERENCES

1. Weber, C. H., and Vincenz, C. (2001) *Trends Biochem. Sci. 26*, 475−481.
2. Fairbrother, W. J., Gordon, N. C., Humke, E. W., O'Rourke, K. M., Starovasnik, M. A., Yin, J. P., and Dixit, V. M. (2001) *Protein Sci. 10*, 1911−1918.
3. Hofmann, K. (1999) *Cell Mol. Life Sci. 55*, 1113−1128.
4. Martin, S. J. (2001) *Trends. Cell Biol. 11*, 188−189.
5. Li, H., and Yuan, J. (1999) *Curr. Opin. Cell Biol. 11*, 261−266.
6. Shi, Y. (2002) *Mol. Cell 9*, 459−470.
7. Shiozaki, E. N., Chai, J., and Shi, Y. (2002) *Proc. Natl. Acad. Sci. U.S.A. 99*, 4197−4202.
8. Qin, H., Srinivasula, S. M., Wu, G., Fernandes-Alnemri, T., Alnemri, E. S., and Shi, Y. (1999) *Nature 399*, 549−557.
9. McCarthy, J. V., Ni, J., and Dixit, V. M. (1998) *J. Biol. Chem. 273*, 16968−16975.
10. Inohara, N., del Peso, L., Koseki, T., Chen, S., and Nunez, G. (1998) *J. Biol. Chem. 273*, 12296−12300.
11. Thome, M., Hofmann, K., Burns, K., Martinon, F., Bodmer, J. L., Mattmann, C., and Tschopp, J. (1998) *Curr. Biol. 8*, 885−888.
12. Kobayashi, K., Inohara, N., Hernandez, L. D., Galan, J. E., Nunez, G., Janeway, C. A., Medzhitov, R., and Flavell, R. A. (2002) *Nature 416*, 194−199.
13. Jeyaseelan, S. (2002) *Trends Microbiol. 10*, 356.
14. Zhou, P., Chou, J., Olea, R. S., Yuan, J., and Wagner, G. (1999) *Proc. Natl. Acad. Sci. U.S.A. 96*, 11265−11270.
15. Vaughn, D. E., Rodriguez, J., Lazebnik, Y., and Joshua-Tor, L. (1999) *J. Mol. Biol. 293*, 439−447.
16. Day, C. L., Dupont, C., Lackmann, M., Vaux, D. L., and Hinds, M. G. (1999) *Cell Death Differ. 6*, 1125−1132.
17. Chou, J. J., Matsuo, H., Duan, H., and Wagner, G. (1998) *Cell 94*, 171−180.
18. Humke, E. W., Shriver, S. K., Starovasnik, M. A., Fairbrother, W. J., and Dixit, V. M. (2000) *Cell 103*, 99−111.
19. Jeong, E. J., Bang, S., Lee, T. H., Park, Y. I., Sim, W. S., and Kim, K. S. (1999) *J. Biol. Chem. 274*, 16337−16342.
20. Eberstadt, M., Huang, B., Chen, Z., Meadows, R. P., Ng, S. C., Zheng, L., Lenardo, M. J., and Fesik, S. W. (1998) *Nature 392*, 941−945.
21. Xiao, T., Towb, P., Wasserman, S. A., and Sprang, S. R. (1999) *Cell 99*, 545−555.
22. Chan, C. K., Hu, Y., Takahashi, S., Rousseau, D. L., Eaton, W. A., and Hofrichter, J. (1997) *Proc. Natl. Acad. Sci. U.S.A. 94*, 1779−1784.
23. Mines, G. A., Pascher, T., Lee, S. C., Winkler, J. R., and Gray, H. B. (1996) *Chem. Biol. 3*, 491−497.
24. Kragelund, B. B., Robinson, C. V., Knudsen, J., Dobson, C. M., and Poulsen, F. M. (1995) *Biochemistry 34*, 7217−7224.
25. Kragelund, B. B., Hojrup, P., Jensen, M. S., Schjerling, C. K., Juul, E., Knudsen, J., and Poulsen, F. M. (1996) *J. Mol. Biol. 256*, 187−200.
26. Huang, G. S., and Oas, T. G. (1995) *Biochemistry 34*, 3884−3892.
27. Burton, R. E., Huang, G. S., Daugherty, M. A., Fullbright, P. W., and Oas, T. G. (1996) *J. Mol. Biol. 263*, 311−322.
28. Ferguson, N., Capaldi, A. P., James, R., Kleanthous, C., and Radford, S. E. (1999) *J. Mol. Biol. 286*, 1597−1608.
29. Gorski, S. A., Capaldi, A. P., Kleanthous, C., and Radford, S. E. (2001) *J. Mol. Biol. 312*, 849−863.
30. Capaldi, A. P., Shastry, M. C., Kleanthous, C., Roder, H., and Radford, S. E. (2001) *Nat. Struct. Biol. 8*, 68−72.
31. Ferguson, N., Li, W., Capaldi, A. P., Kleanthous, C., and Radford, S. E. (2001) *J. Mol. Biol. 307*, 393−405.
32. Capaldi, A. P., Kleanthous, C., and Radford, S. E. (2002) *Nat. Struct. Biol. 9*, 209−216.

33. Marianayagam, N. J., Khan, F., Male, L., and Jackson, S. E. (2002) *J. Am. Chem. Soc. 124*, 9744−9750.
34. Jackson, S. E. (1998) *Fold. Des. 3*, R81−91.
35. Plaxco, K. W., Simons, K. T., and Baker, D. (1998) *J. Mol. Biol. 277*, 985−994.
36. Plaxco, K. W., Simons, K. T., Ruczinski, I., and Baker, D. (2000) *Biochemistry 39*, 11177−11183.
37. McLachlan, A. D. (1980) *Nature 285*, 267−268.
38. Boissinot, M., Karnas, S., Lepock, J. R., Cabelli, D. E., Tainer, J. A., Getzoff, E. D., and Hallewell, R. A. (1997) *EMBO J. 16*, 2171−2178.
39. Getzoff, E. D., Tainer, J. A., Stempien, M. M., Bell, G. I., and Hallewell, R. A. (1989) *Proteins 5*, 322−336.
40. Rajini, B., Shridas, P., Sundari, C. S., Muralidhar, D., Chandani, S., Thomas, F., and Sharma, Y. (2001) *J. Biol. Chem. 276*, 38464−38471.
41. Rudolph, R., Siebendritt, R., Nesslauer, G., Sharma, A. K., and Jaenicke, R. (1990) *Proc. Natl. Acad. Sci. U.S.A. 87*, 4625−4629.
42. Hamill, S. J., Cota, E., Chothia, C., and Clarke, J. (2000) *J. Mol. Biol. 295*, 641−649.
43. Capaldi, A. P., Ferguson, S. J., and Radford, S. E. (1999) *J. Mol. Biol. 286*, 1621−1632.
44. Jones, S., Reader, J. S., Healy, M., Capaldi, A. P., Ashcroft, A. E., Kalverda, A. P., Smith, D. A., and Radford, S. E. (2000) *Biochemistry 39*, 5672−5682.
45. Reader, J. S., Van Nuland, N. A., Thompson, G. S., Ferguson, S. J., Dobson, C. M., and Radford, S. E. (2001) *Protein Sci. 10*, 1216−1224.
46. Richardson, J. S., Richardson, D. C., Tweedy, N. B., Gernert, K. M., Quinn, T. P., Hecht, M. H., Erickson, B. W., Yan, Y., McClain, R. D., Donlan, M. E., et al. (1992) *Biophys. J. 63*, 1185−1209.
47. Zhang, C., and Kim, S. H. (2000) *Proteins 40*, 409−419.
48. Hazes, B., and Hol, W. G. (1992) *Proteins 12*, 278−298.
49. Hemmingsen, J. M., Gernert, K. M., Richardson, J. S., and Richardson, D. C. (1994) *Protein Sci. 3*, 1927−1937.
50. Nishimura, C., Uversky, V. N., and Fink, A. L. (2001) *Biochemistry 40*, 2113-2128.
51. Dominy, B. N., Perl, D., Schmid, F. X., and Brooks, C. L., 3rd. (2002) *J. Mol. Biol. 319*, 541−554.
52. Shaw, K. L., Grimsley, G. R., Yakovlev, G. I., Makarov, A. A., and Pace, C. N. (2001) *Protein Sci. 10*, 1206−1215.
53. Pace, C. N., Shirley, B., and Thompson, J. (1989) in *Protein Structure, A Practical Approach* (Creighton, T. E., Ed.) pp 311−330, IRL Press, New York.
54. Edelhoch, H. (1967) *Biochemistry 6*, 1948−1954.
55. Royer, C. A., Mann, C. J., and Matthews, C. R. (1993) *Protein Sci. 2*, 1844−1852.
56. Santoro, M. M., and Bolen, D. W. (1988) *Biochemistry 27*, 8063−8068.
57. Schmid, F. X. (1986) *Methods Enzymol. 131*, 70−82.
58. Schmid, F. X. (1983) *Biochemistry 22*, 4690−4696.
59. Pappenberger, G., Aygun, H., Engels, J. W., Reimer, U., Fischer, G., and Kiefhaber, T. (2001) *Nat. Struct. Biol. 8*, 452−458.
60. Druilhe, A., Srinivasula, S. M., Razmara, M., Ahmad, M., and Alnemri, E. S. (2001) *Cell Death Differ. 8*, 649−657.
61. Lee, S. H., Stehlik, C., and Reed, J. C. (2001) *J. Biol. Chem. 276*, 34495−34500.
62. Alonso, D. O., and Dill, K. A. (1991) *Biochemistry 30*, 5974−5985.
63. Schellman, J. A. (1978) *Biopolymers 17*, 1305−1322.
64. Myers, J. K., Pace, C. N., and Scholtz, J. M. (1995) *Protein Sci. 4*, 2138−2148.
65. Perl, D., and Schmid, F. X. (2001) *J. Mol. Biol. 313*, 343−357.
66. Lee, K. K., Fitch, C. A., and Garcia-Moreno, E. B. (2002) *Protein Sci. 11*, 1004−1016.
67. Baldwin, R. L. (1996) *Biophys J. 71*, 2056−2063.
68. Record, M. T., Jr., Zhang, W., and Anderson, C. F. (1998) *Adv. Protein Chem. 51*, 281−353.
69. Jackson, S. E., and Fersht, A. R. (1991) *Biochemistry 30*, 10428−10435.
70. Chen, B. L., Baase, W. A., Nicholson, H., and Schellman, J. A. (1992) *Biochemistry 31*, 1464−1476.
71. Kiefhaber, T., Quaas, R., Hahn, U., and Schmid, F. X. (1990) *Biochemistry 29*, 3053−3061.
72. Brandts, J. F., Halvorson, H. R., and Brennan, M. (1975) *Biochemistry 14*, 4953−4963.
73. Kiefhaber, T. (1995) *Methods Mol. Biol. 40*, 313−341.
74. Munoz, V., and Serrano, L. (1994) *Nat. Struct. Biol. 1*, 399−409.
75. Baldwin, R. L. (1996) *Fold Des. 1*, R1−8.
76. Creighton, T. E. (1994) *Nat. Struct. Biol. 1*, 135−138.
77. Heidary, D. K., Gross, L. A., Roy, M., and Jennings, P. A. (1997) *Nat. Struct. Biol. 4*, 725−731.
78. Hosszu, L. L., Craven, C. J., Parker, M. J., Lorch, M., Spencer, J., Clarke, A. R., and Waltho, J. P. (1997) *Nat. Struct. Biol. 4*, 801−804.

BI0340752